Angular Distributions of Ground-State Protons from $B^{10}+D$*

W. C. REDMAN†
Sloane Physics Laboratory, Yale University, New Haven, Connecticut‡
(Received March 13, 1950)

The angular distributions of the ground-state protons resulting from the deuteron bombardment of B^{10} has been investigated at six energies in the 1- to 4-Mev interval. The reaction protons were recorded photographically at all angles from 5° to 165° and their distribution was determined by microscopic examination of the photographic emulsion. The resulting intensity variation with angle can be expressed within experimental error as a second-order Legendre polynomial series for all energies except the highest, for which a fourth-order series is required. *S*-wave deuterons predominate in producing this reaction, but *p*-wave effects occur even for the lowest energy distribution studied. *D*-wave contributions are noticed for deuteron energies above 3 Mev. The behavior of the coefficients in the series representation shows that several broad overlapping resonance levels, of both even and odd parity, in the compound nucleus probably enter into this reaction.

I. INTRODUCTION

INCREASING attention has been given recently to angular distribution studies as a fruitful approach to the field of nuclear spectroscopy. Recent work on d, p reactions by Heydenburg, Inglis, and co-workers[1] has indicated that an investigation of other similar reactions may furnish useful information.

The high energy release, $Q=9.14$ Mev, in the $B^{10}(d, p)B^{11}$ reaction makes it convenient for such a study. Because of the high excitation energy of the $B^{10}+D$ system, about 25 Mev for zero energy bombarding deuterons, no abrupt changes in the distribution with varying energy are to be expected, a favorable factor in view of the appreciable energy spread of the Yale cyclotron beam. In spite of this limitation, a knowledge of the trend in the angular distribution with increasing bombardment energy and information about the nature of this particular reaction should result. Photographic detection provides good discrimination against the prolific neutron yield from competing reactions, and through all-angle recording the presence or absence of appreciable fine structure in these distributions can be determined.

II. APPARATUS AND PRELIMINARY TESTS

A schematic plan of the combination bombardment chamber and angular distribution camera used is shown in Fig. 1. Similar chambers described by Wilkins[2] and Rubin[3] have influenced the design. This chamber is mounted past the magnetic deflector of the cyclotron with the photographic plates in a plane parallel to the direction of the stray magnetic field (<100 oersteds) in this region. The deuteron beam is stopped down to reduce its area, and is finally collimated into a $\frac{3}{16}$-in. diameter stream which strikes a solid target. The target support is attached to a Stupakoff metal-glass seal which passes through the base-plate of the chamber. Thus the target is insulated from the chamber which in turn is insulated from the cyclotron by Lucite bushings surrounding the bolts. The target mounting is a C-shaped, sandwich-type holder, permitting the observation of reaction particles emitted from both faces of the target. Beyond the target in the beam path is located a small window. This contains a fluorescent screen used for obtaining proper alignment of the chamber. Aluminum absorbers are interposed in the beam path to vary the bombarding energy. A fraction of the reaction particles pass through aluminum absorber foils mounted over an extended slit in the inner cylinder and enter the photographic emulsion at small angles with respect to the plane of the plates. Three 1×3-in. Ilford 100μ-type *C*-2 plates record these emitted particles at all angles from 0° to ~170° in the emulsion plane. The plates fit tightly in a holder which is positioned slightly below and parallel to the axis of the beam. In construction, all components were located relative to the fixed base-plate.

Solid targets of B_2O_3 from $\frac{1}{2}$ to 1 cm air equivalent were prepared by evaporating boracic acid, H_3BO_3, from a tungsten filament onto 5-cm air equivalent gold foil. Because of the long range of the end-group protons from $B^{10}(d, p)B^{11}$, these protons are easily separated from the oxygen and other boron charged particle groups by aluminum absorbers interposed between the target and photographic plates. Photographic plates are comparatively insensitive to the emitted neutrons due to the dependence on the neutron-proton scattering cross section for the production of recoil proton tracks. At the higher energies of bombardment the deuteron beam which passes through the target backing is absorbed in a gold foil mounted on the inner cylinder.

Ilford emulsions showed less tendency to crack or peel from their glass backing than did other similar

* Part of a dissertation presented to the Faculty of the Graduate School of Yale University in candidacy for the degree of Doctor of Philosophy.
† Now at Argonne National Laboratory, Chicago, Illinois.
‡ Assisted by the joint program of the ONR and AEC.
[1] N. P. Heydenburg and D. R. Inglis, Phys. Rev. **73**, 230 (1948); Heydenburg, Inglis, Whitehead, and Hafner, Phys. Rev. **75**, 1147 (1949); Krone, Hanna, and Inglis, Phys. Rev. **75**, 335(A) (1949); I. Resnick and S. S. Hanna, Phys. Rev. **76**, 168(A) (1949).
[2] T. R. Wilkins, Phys. Rev. **60**, 365 (1941).
[3] S. Rubin, Phys. Rev. **72**, 1176 (1947).

plates tested for performance during lengthy use in the evacuated chamber. For uniform development throughout such thick emulsions, the normal procedure is to soak the plates in developer at a low temperature before processing. However, to enhance the development of the initial part of the proton tracks for which the grain density is least and to supress the recoil proton tracks under the emulsion surface, this presoaking was eliminated in the plate processing procedure.

In order to check the range-energy relation for these emulsions, to test the techniques used to process the plates and observe the track distribution, and to determine the purity of the B_2O_3 targets used, the stopping power was determined for proton groups of three energies. The results were in essential agreement with published values[4] and there was no indication of extraneous tracks.

III. EXPERIMENTAL PROCEDURE

The aluminum foils necessary to reduce the incident deuteron energy to the desired value were inserted in the beam path. In addition to the gold foil to absorb the deuterons transmitted by the target backing, aluminum absorber thicknesses sufficient to cut off all emitted charged particles except the end-group protons were mounted on the inner cylinder. Because of the large variation of range with angle, increasing absorption was introduced with decreasing angle so that only the single group of protons would be recorded in the emulsion. Since data are lost at small angles with respect to the target and in the vicinity of the discontinuities in absorption, two sets of plates were exposed for each bombarding energy with the target at 70° and 110° with respect to the incident beam direction and the discontinuities at different angles. A normalization of the two exposures could be effected with data from angular regions common to the two sets of plates.

TABLE I. Summary of the six bombardment runs.

Mean deuteron energy (Mev)	Target thickness (cm air equiv.)	Beam axis -emulsion plane separation (cm)	Total tracks counted	Number of angles of observation
1.06	0.62	0.95	10620	17
1.50	0.81	1.41	11616	14
1.71	0.58	0.95	11137	17
2.36	0.92	0.95	12607	16
3.06	0.57	0.95	15953	19
3.68	0.94	0.95	9844	13

After development, the original position of the plates was duplicated and a very light grid of polar coordinates was scribed directly onto the emulsion surface. For each angle the end-group proton track density was determined microscopically over an average area 1 mm wide and 10 mm in length along the radial line. Each eyepiece of the binocular microscope contained a glass disk with rulings coincident with the objective image. On one disk was ruled a scale, useful for measuring proton track lengths, on the other a grid which divided the field of view into small squares, thereby simplifying the track density determination. A 43X achromatic objective in conjunction with 5X eyepieces provided the most convenient combination for the proton track lengths measured. Only those tracks satisfying certain requirements were counted. The track had to start at the surface of the emulsion, make no more than a 5° angle with the radial direction and be of the proper length. Tracks starting below the emulsion surface cannot be those of charged particles emitted by the target. The limiting angle acceptable for a track was decided from a maximum half-angle of 3.5° subtended

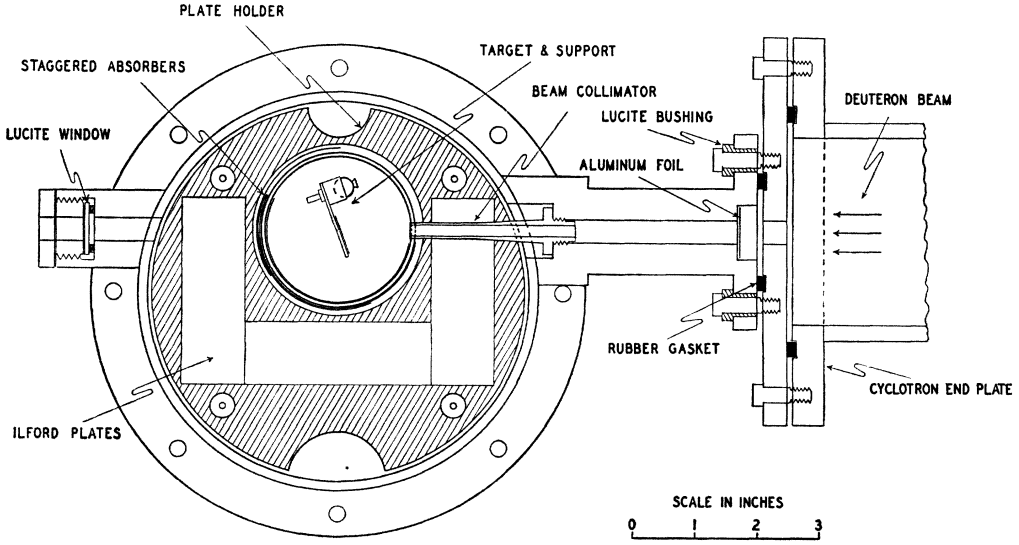

FIG. 1. Plan of the combination bombardment chamber and angular distribution camera.

[4] Lattes, Fowler, and Cuer, Proc. Phys. Soc. London **59**, 883 (1947).

by the source at a point on the emulsion and an additional allowance of 1.5° for small-angle scattering of the proton by the gold and aluminum absorbers. The allowable length for the tracks was determined from a numbers-range plot of the first 150 tracks observed at a particular angle. It was then necessary only to count additional tracks satisfying the above criteria. The angular width of the area counted was always less than 2°.

IV. DATA AND ERRORS

Distribution measurements were made at six energies as given in Table I. Included in this table are the mean effective deuteron energy, the target thickness in cm air equivalent, the separation between beam axis and emulsion plane, the total number of end-group proton tracks counted, and the total number of angles for which the yield was determined. An average of 748 tracks for each of 16 angles, representing about 0.75 percent of the proton tracks recorded on the plates, constituted the distribution data determined at each energy. Normally, data were obtained at 15° intervals from 0° to 165° in the emulsion plane, and at such intermediate angles as were needed to define the distribution curve shape. Not included in Table I are two background runs made at full beam energy to test the track contribution

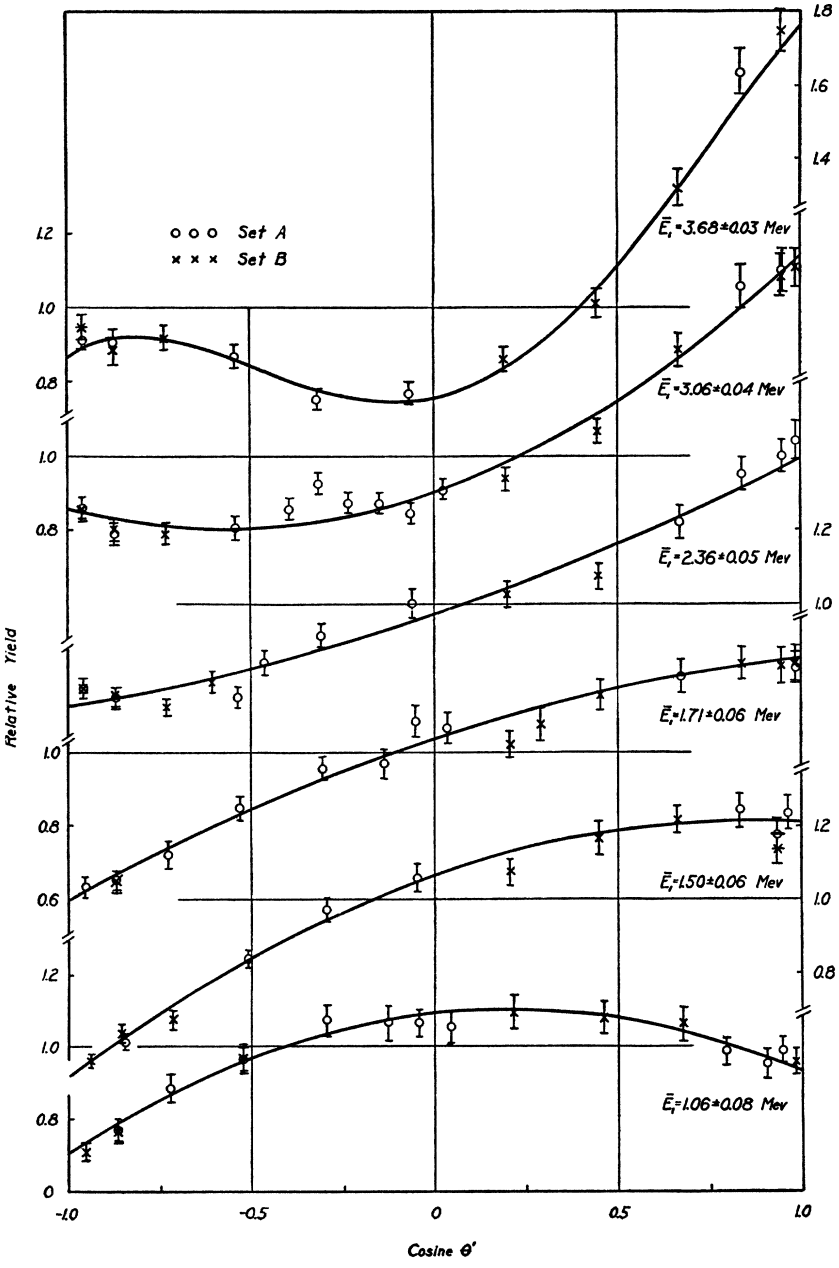

FIG. 2. Relative yield of the end-group protons from $B^{10}+D$ as a function of the cosine of the angle between the incident deuterons and emitted protons plotted in the center-of-mass system for various deuteron energies. The error limits indicated for the individual angular yields are those of statistical origin only. The coefficients listed in Table II were used to draw the curves, using $I(\mu)=\Sigma_i a_i P_i(\mu)$ up to $i=4$ for the highest energy distribution and $i=2$ for the other five.

TABLE II. Coefficients in the Legendre polynomial series representation of experimental angular distribution curves, normalized to a value of unity for a_0.

Mean deuteron energy (Mev)	Values of $a_i=\frac{1}{2}(2i+1)\int_{-1}^{+1} I(\mu)P_i(\mu)d\mu$ from experimental distribution curves							
	a_0	a_1	a_2	a_3	a_4	a_5	a_6	a_7
1.06	1.000	+0.111	−0.180	+0.007	−0.041	−0.010	−0.082	−0.023
1.50	1.000	+0.345	−0.134	+0.003	−0.046	−0.039	−0.091	−0.056
1.71	1.000	+0.325	−0.074	−0.017	−0.042	−0.029	−0.096	−0.054
2.36	1.000	+0.334	+0.057	+0.028	+0.033	−0.075	−0.150	−0.052
3.06	1.000	+0.341	+0.198	+0.041	−0.053	−0.089	−0.147	−0.061
3.68	1.000	+0.352	+0.414	+0.094	−0.101	−0.043	−0.193	−0.111

by the cyclotron, neutrons from the bombarded target and contaminants introduced in handling the target. No appreciable effect was observed.

The data obtained from the microscopic examination of the photographic plates must be related to $\sigma_{K,\theta}$, the cross section per unit solid angle for the emission of a particular type of particle K at an angle θ. Since the emulsion is at an angle with respect to the normal to the radial direction, the track density is proportional to r^{-3}, where r is the distance from the target center to a point on the emulsion. If N end-group proton tracks are counted in an area of width w extending from r_1 to r_2, the cross section is given by

$$\sigma_{K,\theta}=C(N/w)r_2^2r_1^2/(r_2^2-r_1^2). \quad (1)$$

The constant of proportionality, C, is dependent upon the number of target nuclei bombarded, the deuteron flux, the duration of bombardment, and the axis-plane separation. Actually the data are obtained at an angle ϕ in the plane of the emulsion. In terms of known quantities, θ is given by

$$\sin\theta=[\sin^2\phi+(h/d)^2]^{\frac{1}{2}}[1+(h/d)^2]^{-\frac{1}{2}}. \quad (2)$$

Here d is the distance in the emulsion plane from the point below the target center to the center of the area in which the tracks are observed, and h is the separation between the beam axis and the emulsion plane. For convenience in analyzing the resulting distributions, the data were expressed in the center-of-mass coordinate system, using the standard transformations for the angular coordinate and yield per unit solid angle.[5]

The largest error involved in these measurements is statistical, and it is the most difficult to reduce in the photographic method. For example, doubling the number of tracks counted would reduce the root-mean-square error, amounting to about ±4 percent here, by less than one-third.

The proton intensity deduced on the assumption that the angle of incidence for the protons is $\arcsin(h/r)$ would be in error by $100\gamma r/h$ percent if the emulsion surface is inclined at some angle γ with respect to the plane of the plate holder. Such a tilt in the emulsion plane can occur if the surface is not smooth or the glass backing is not uniform. An optical test of the emulsion smoothness showed that the variations were of the order of a wave-length of green light per cm, except at the edges which were avoided in these measurements. By counting tracks over a radial strip the effect of surface variations was to some extent further decreased. The plate thickness varied from plate to plate, but was essentially constant for a given plate. An upper limit of ±3 percent error introduced through this possible tilt of the emulsion surface seems reasonable, plus a ±1 percent error due to the change in h caused by the variation in plate thickness. For the run at 1.50 Mev, h was increased from 0.95 to 1.41 cm to reduce these errors.

The Coulomb scattering of the end-group protons by the gold target backing and aluminum absorbers will modify the actual intensity. This spreading of the proton flux initially headed for a part of the photographic plate is compensated for in part by the scattering of other protons into that region. As some large-angle scattering will always occur, this compensation will never be complete and will depend on the conditions of scatter-

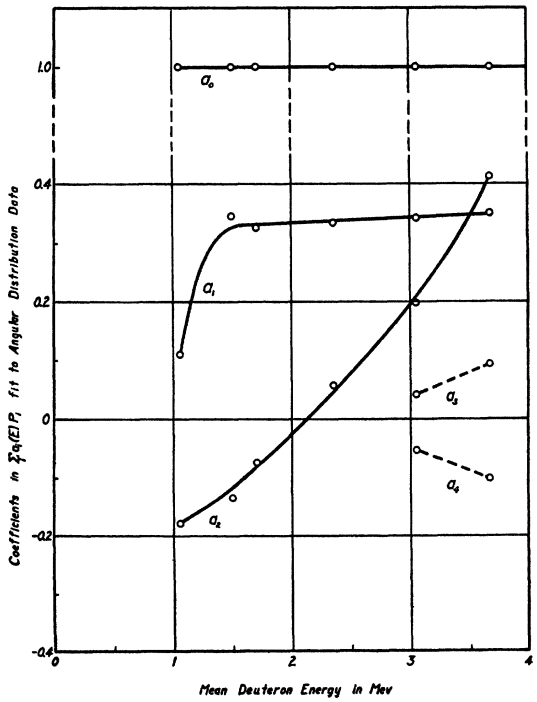

FIG. 3. Coefficients in the $\Sigma_i a_i(E)P_i(\mu)$ fit to the angular distribution data relative to a_0 plotted as a function of the deuteron mean energy.

[5] See L. I. Schiff, *Quantum Mechanics* (McGraw-Hill Book Company, Inc., New York, 1949), pp. 97–100.

ing, such as gold and aluminum path thickness and proton energy, prevailing at the adjacent angles. Each measured intensity will be reduced somewhat, but only the differential effect is of primary importance as an error source. Consideration of the effect of multiple small-angle scattering as treated by Breit, Thaxton, and Eisenbud,[6] and observation of the fraction of proton tracks of proper length which did not satisfy the ± 5 percent requirement place ± 2 percent as a reasonable estimate of the error introduced by not correcting each measured intensity for the effect of Coulomb scattering of the protons.

The selection of the extent of the proton group from the numbers-range curve and the measurement of the radial boundaries r_1 and r_2 of the area counted each introduces an error of the order of two percent. The effect of a possible displacement of the target source from its assumed position in the chamber and of the effective center due to non-uniformity of beam flux and/or target thickness is estimated as a possible ± 2 percent error for each. The scattering of protons out of the emulsion, the recoil proton contribution, the warp and creep of the emulsion and the assumption of a point source for the calculations each give rise to less than a ± 1 percent error.

The total expected error in each of the values of the relative intensity, compounded from the estimates of the effect of the individual sources of error discussed above, is ± 7 percent. In a number of these cases a pessimistic evaluation was made, while for others the error assigned was just a reasonable estimate. This ± 7 percent will about double the error limits shown in the graph of the data, as discussed below. There, only error of statistical origin is indicated.

The main uncertainty in the angular coordinate arises from the mechanics of scribing the coordinates on the emulsion surface, and the possibility of displacement, actual or effective, of the target center from the location assumed. Consequently, an uncertainty of $\pm\frac{1}{2}°$ is assigned to the angular coordinate.

V. DISCUSSION OF RESULTS

The observed intensity per unit solid angle as a function of the cosine of the angle is plotted in Fig. 2 for the center-of-mass system. Intensity values at the two angles common to the sets of data A and B are used to normalize the data at each energy. The error limits given for the six energies at which the distributions were observed are those resulting from the uncertainty in the measurement of the full beam energy.

In the wave mechanical representation of a nuclear reaction system the angular dependence of the emitted particles occurs in terms of Legendre polynomials. It is a well-known fact in the theory of Legendre functions that in the expansion of the intensity I as

$$I(\mu)=\Sigma_i a_i(E)P_i(\mu)$$

in a series of Legendre polynomials the energy-dependent coefficients a_i are given by

$$a_i=\tfrac{1}{2}(2i+1)\int_{-1}^{+1} I(\mu)P_i(\mu)d\mu. \tag{3}$$

Here μ is the cosine of the angle between the directions of the incident and emitted particles. A curve was drawn through the experimental points at each energy, and the values from this curve were used in a 20-part numerical integration to determine these coefficients. This method of fitting the distribution is noteworthy, for it is insensitive to the individual values or the detailed shape of the experimental curve. However, a certain amount of accidental personal judgment enters the operation of drawing the curve and the values of the a_i for higher values of the index i may therefore be inaccurate.

The values of a_i thus determined are given in Table II, normalized to a value of unity for a_0. As the values of a_3 and a_4 for all energies except the highest were less than the experimental error of ± 7 percent, a second-order series in $P(\mu)$ was used to represent these distributions. Two additional terms were used to fit the experimental intensity distribution at the highest energy. The values of the coefficients listed in Table II were used to draw the curves shown in Fig. 2, using $I(\mu)=\Sigma_i a_i P_i(\mu)$ up to $i=4$ for the highest energy distribution and $i=2$ for the other five. The agreement of these curves with the experimental data indicates that higher order Legendre polynomials are not needed. The magnitude of a_6 in each case is perhaps indicative of a consistent manner of terminating the curves drawn through the experimental points. For higher values of i, any slight irregularity in the curve drawn is magnified by the $\frac{1}{2}(2i+1)$ factor. The behavior of the coefficients in the analytical representation of the observed distributions is shown in Fig. 3. The values of a_3 and a_4 for $E=3.06$ Mev, although not used in the curve fitting because they are less than the experimental error, are included to show a possible trend.

The asymmetry of the observed distributions indicates that incident deuterons having both even and odd angular momentum values are effective in producing this reaction. The successful fit of the data with a second-order power series in angle for all but the highest energy implies that only s and p deuterons contribute appreciably to the reaction at low energies. Because the possible initial, compound and final quantum states for the $B^{10}(d, p)B^{11}$ reaction are so numerous, a unique explanation of the energy variation of the coefficients appears to be difficult.

At the lowest bombardment energy, the incident s-wave contribution predominates in the observed distribution. With increasing energy the incident p-wave contribution becomes sizeable, and for the highest energy d-wave effects in the distribution are

[6] Breit, Thaxton, and Eisenbud, Phys. Rev. 55, 1018 (1939).

noticeable. It seems reasonable to assume that contributions by incident f-waves are negligible in the energy range covered, in view of the small effect observed for d-waves. The absence of abrupt changes in the distributions observed indicates that probably several broad overlapping resonances in the compound nucleus participate in this reaction, as anticipated because of the high degree of excitation of the $B^{10}+D$ system. Due to the observed asymmetry, these levels must differ in parity.

It is a sincere pleasure to acknowledge the guidance and encouragement provided by Professor R. F. Humphreys throughout this investigation. The many informative discussions with Professor G. Breit on the interpretation of angular distribution data are appreciated.

PHYSICAL REVIEW VOLUME 79, NUMBER 1 JULY 1, 1950

Low Energy Neutron Resonance Scattering and Absorption

S. P. HARRIS, C. O. MUEHLHAUSE, AND G. E. THOMAS
Argonne National Laboratory, Chicago, Illinois

(Received February 2, 1950)

Low energy neutron resonance absorption and scattering integrals have been measured, and resonance scattering fractions, Γ_n/Γ, have been determined for about thirty elements. Lightweight odd Z—even N and even Z—odd N isotopes are shown to have similar resonance phenomena. Correlations of level density and scattering fraction with atomic weight and nuclear type are presented.

I. INTRODUCTION

STRONG resonance absorption of slow neutrons has been observed for many elements since the discovery of neutron resonance phenomena by Fermi and others in 1936. The neutron spectrum of energies greater than thermal but less than 100 kev is usually referred to as the "epi-cadmium region," the "S-resonance region," or simply as the "resonance region." At these energies neutron scattering is almost entirely S-wave scattering. Though the existence of neutron resonance scattering was known experimentally and appreciated theoretically[1] as early as 1937, it was not until 1946 that Goldhaber[2,3] showed that in the case of $_{25}Mn^{55}$ neutrons at resonance ($\sim$300 ev) were scattered much more frequently than they were absorbed. Since that time, additional nuclei have been found which possess primarily scattering resonances. Some of these are: (a) $_{27}Co^{59}$ (115 ev)[4] 94 percent scattering; (b) $_{62}Sm^{152}$ (10 ev)[5] 66 percent scattering; (c) $_{74}W^{186}$ (18 ev)[6,7] 81 percent scattering.

The contribution to the total neutron cross section of scattering and absorption near resonance is given in the following simplified version of the Breit-Wigner formula[1]

$$\sigma_T(E)=\sigma_p+4\pi\lambda_0^2 g\frac{\Gamma_n^2}{\Gamma^2}\frac{1}{1+[(E-E_0)/(\Gamma/2)]^2}+4\pi\lambda_0^2 g\frac{\Gamma_n\Gamma_\gamma}{\Gamma^2}\frac{1}{1+[(E-E_0)/(\Gamma/2)]^2}$$

where: $\sigma_T(E)$—total neutron cross section at energy E; σ_P—potential scattering cross section; E_0—energy of resonance; λ_0—neutron wave-length (divided by 2π) at the resonance energy E_0; Γ_n—neutron resonance width at half-maximum; Γ_γ—γ-ray resonance width at half-maximum; Γ—total resonance width $(\Gamma_n+\Gamma_\gamma)$ at half-maximum g—$\frac{1}{2}[1\pm(1/2i+1)]$—statistical weight factor where "i" is the spin of the target (i.e., initial) nucleus. The second term in σ_T is the resonance scattering cross section, σ_{rs}, and the third term is the resonance absorption cross section, σ_{ra}.

The epi-cadmium neutron spectrum usually encountered (e.g., from a pile) is distributed in energy as $1/E$. An important measurable quantity, then, is the average epi-cadmium cross section for such a flux. In place of this, however, one usually considers a quantity proportional to the average epi-cadmium cross section, namely the resonance integral, Σ. This is defined as $\Sigma=\int\sigma_{res}dE/E$. Using the Breit-Wigner expressions for σ_{rs} and σ_{ra}, it can be readily shown that

$$\Sigma_s=(\pi/2)(4\pi\lambda_0^2 g\Gamma/E_0)\Gamma_n^2/\Gamma^2 \quad \text{res. scatt. integral,}$$
$$\Sigma_a=(\pi/2)(4\pi\lambda_0^2 g\Gamma/E_0)\Gamma_n\Gamma_\gamma/\Gamma^2 \quad \text{res. abs. integral,}$$
$$\Sigma_s+\Sigma_a=(\pi/2)(4\pi\lambda_0^2 g\Gamma/E_0)\Gamma_n/\Gamma \quad \text{total res. integral,}$$

[1] H. A. Bethe and G. Placzek, Phys. Rev. **51**, 450 (1937).
[2] M. Goldhaber and A. A. Yalow, Phys. Rev. **69**, 47(A) (1946).
[3] N. H. Barbre and M. Goldhaber, Phys. Rev. **71**, 141(A) (1947).
[4] Harris, Langsdorf, and Seidl, Phys. Rev. **72**, 866 (1947).
[5] M. Goldhaber and A. W. Sunyar, Phys. Rev. **76**, 189(A) (1949).
[6] M. Goldhaber and L. L. Lowry, Phys. Rev. **76**, 189(A) (1949).
[7] S. P. Harris and C. D. Muehlhause, Phys. Rev. **76**, 189(A) (1949).